

## Analytical model of transient thermal effect on convectional cooled end-pumped laser rod

KHALID S SHIBIB\*, MOHAMMAD A MUNSHID and  
KADIM A HUBITER

Department of Laser and Optoelectronics Engineering, University of Technology, Baghdad, Iraq

\*Corresponding author. E-mail: assprofkh@yahoo.com

MS received 10 March 2013; revised 22 June 2013; accepted 4 July 2013

DOI: 10.1007/s12043-013-0600-x; ePublication: 26 September 2013

**Abstract.** The transient analytical solutions of temperature distribution, stress, strain and optical path difference in convectional cooled end-pumped laser rod are derived. The results are compared with other works and good agreements are found. The effects of increasing the edge cooling and face cooling are studied. It is found that an increase in the edge cooling has significant effect on reducing the maximum temperature that can be reached in the laser rod but it has no effect on the value of optical path difference. It is also found that increasing this type of cooling significantly reduces the time required to reach the thermal equilibrium with a slight increase in the max. tensile hoop stress that can be reached as the cooling increases. On the other hand, increase in face cooling reduces the response time, optical path difference and the maximum temperature that can be reached in the laser rod but a significant increase in the max. tensile hoop stress is observed. A matching between the advantages of these two type of cooling may be useful for a designer.

**Keywords.** Analytical solution; heat transfer; laser rod; convectional cooling; thermal stress; optical path difference.

PACS Nos 42.55.Xi; 44.05.+e

### 1. Introduction

Limitation on power scalability from an end-pumped system is its major drawback. End-pumped solid-state lasers are attractive because of their high efficiency and good beam quality [1]. The factor that limits the increase in the output power from solid-state laser system is the heat that can be generated by the process of laser generation. Excessive heat may cause thermal stress and thermal lens which may degrade the laser output, degrade the beam quality and at excessive thermal stress, it may lead to medium break [1–4]. One of the most obvious phenomena indicating the excessive heat generation is the strong thermal lensing. The three factors that contribute to this phenomenon in a pumped laser medium are: (1) the change of refractive index which is occurred due to

the gradient in the temperature distribution, (2) the thermal stress effect on the refractive index, (3) the change of the path of light due to thermal expansion [5]. In most cases, the last factor mentioned above is insignificant and can be ignored. So the gradient of temperature in a laser rod causes a thermal distortion of the laser beam due to the temperature- and stress-dependent variation of the refractive index which can be physically presented as optical path difference.

Due to its relative ease, clear physical meaning and compactness, analytical solution is still preferable wherever possible. Many works are devoted to such problems. Bernhardt *et al* [6] studied an analytical solution of transient one-dimensional temperature distribution and stress profile in longitudinally pumped laser rod. Tian *et al* [7] presented a transient one-dimensional analytical model of thermal effect in CW end-pumped laser rod. Peng Shi *et al* [5] derived sem-analytical thermal analysis of thermal focal length in laser rod using the method of separation of variable for solving multi-dimensional heat equation. Feng Huang *et al* [8] solved analytically the temperature and stress distribution in an end-pumped heat capacity disk laser. Shibib [3,9] derived a transient analytical solution of temperature and Tresca failure stress in CW end-pumped laser rod where a minimization in thermal response and stress was predicted. All the previously mentioned works assumed insulated rod facets. In this work the transient axis symmetry heat equation that model the convectionally cooled end-pumped laser rod has been solved analytically using integral transform method and an expression for optical path difference (OPD) has been derived. The resulting analytical solution then applied to an Nd:YAG laser rod and was compared with numerical solutions, good agreements were observed then the induced hoop stress due to temperature gradients was obtained also the effect of convection heat transfer coefficient on hoop stress and the optical path difference were also predicted. To the best of our knowledge, this is the first time that the analytical solution of transient temperature distribution through laser rod that convectionally cooled through its facets and edge was derived.

## 2. Theory

The solution of heat equation in laser rod permits the prediction of temperature distribution which is the first step in determining thermal effects in the laser rod. The transient temperature distribution through the laser rod can be determined by solving the axis symmetry heat equation [10]:

$$\frac{\partial^2 T}{\partial r^2} + \frac{1}{r} \frac{\partial T}{\partial r} + \frac{\partial^2 T}{\partial z^2} + \frac{Q}{k} = \frac{\rho c}{k} \frac{\partial T}{\partial t}, \quad (1)$$

where  $\rho$ ,  $c$ ,  $k$ ,  $T$  are respectively the density in  $\text{kg/m}^3$ , specific heat in  $\text{J/kg}\cdot\text{K}$ , thermal conductivity in  $\text{W/m}\cdot\text{K}$ , and temperature in  $\text{K}$ ,  $r$  and  $z$  are the radial and longitudinal coordinates in  $\text{m}$  and  $Q$  is the heat generation in  $\text{W/m}^3$ . The boundary conditions are (see figure 1):

$$k \left. \frac{\partial T}{\partial r} \right|_{r=r_0} = h_e (T_\infty - T) \quad \text{at } r = r_0, \quad (1a)$$

$$k \left. \frac{\partial T}{\partial z} \right|_{z=0} = h_a (T_\infty - T) \quad \text{at } z = 0, \quad (1b)$$

Convictional cooled end-pumped laser rod

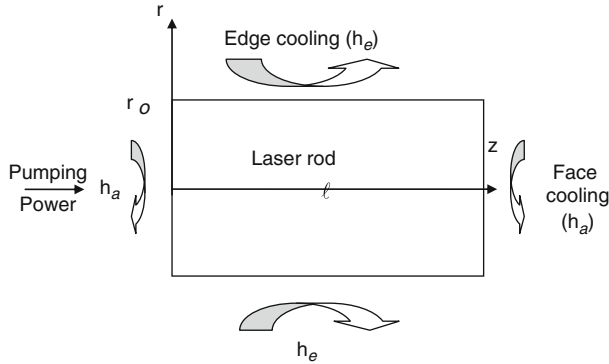


Figure 1. Laser rod and its boundary conditions.

$$-k \left. \frac{\partial T}{\partial z} \right|_{z=l} = h_a(T_\infty - T) \quad \text{at } z = l, \quad (1c)$$

$$\frac{\partial T}{\partial r} = 0 \quad \text{at } r = 0. \quad (1d)$$

Convection boundary conditions are assumed at the facets of the rod where  $h_a$  represents the convection heat transfer coefficient of the naturally cooled facets in  $\text{W/m}^2\cdot\text{K}$ ,  $h_e$  is the edge convection heat transfer coefficient in  $\text{W/m}^2\cdot\text{K}$ ,  $l$  is the length of the rod = 20 mm,  $r_0$  is the outside rod radius = 4.76 mm. The initial and environmental temperatures ( $T_\infty$ ) are equal to  $25^\circ\text{C}$ .

A practical edge cooling is accomplished by mounting the rod in copper heat sink. Heat conductivity was provided by an indium layer between copper and the crystal. The mass flow rate of cooling water was adjusted to provide the required heat transfer coefficient. To increase the face cooling, other than natural cooling, the edge mounted rod is designed to allow direct water cooling of the facets.

Neodymium concentration by atom percent in YAG is limited to 1.0–1.5% and higher doping levels tend to shorten the fluorescent lifetime, increasing absorption coefficient which increases temperatures and its gradient assumes high temperature gradient which causes high stress and strain in the crystal, resulting in poor optical quality [4]. Generally, high doping concentration ( $\sim 1.2\%$ ) is desirable for Q-switch operation because this will lead to high energy storage. For continuous wave operation, a low doping concentration (0.6–0.8%) is usually chosen to obtain good beam quality [4].

The part of the absorbed power that is converted to heat acts as a source of heat generation inside a laser rod. For pumping that has a Gaussian beam distribution, heat generation inside the laser rod can be written as [11]

$$Q = \begin{cases} \frac{2\alpha H_f P_{ab} \exp(-\alpha z) \exp(-2r^2/w_p^2)}{\pi w_p^2 [1 - \exp(-\alpha l)]} & 0 \leq r \leq r_1, t \geq 0 \\ 0 & r_1 \leq r \leq r_0, t \geq 0 \\ 0 & t < 0 \end{cases} \quad (2)$$

where  $\alpha$  is the absorption coefficient ( $\text{m}^{-1}$ ),  $H_f$  is the heat factor and  $P_{ab}$  is the part of the pumping power that is absorbed in the laser rod (W). Mathematically, to include all the pumping power in a beam that has a Gaussian profile, the radius of pumping is taken to be twice bigger than the waist radius (i.e.  $r_1 = 2w_p$ ). The standard solution for eq. (1) can be written as [12]

$$\theta = T - T_\infty = \sum_{m=1}^{\infty} \sum_{p=1}^{\infty} \frac{R_0(\beta_m, r) Z(\eta_p, z)}{N(\beta_m) N(\eta_p)} \exp\left(-\frac{k}{\rho c} (\beta_m^2 + \eta_p^2) t\right) \times \left[ \frac{1}{\rho c} \int_{t'=0}^t \exp\left(\frac{k}{\rho c} (\beta_m^2 + \eta_p^2) t'\right) \bar{g}(\beta_m, \eta_p, t') dt' \right], \quad (3)$$

where

$$\bar{g}(\beta_m, \eta_p, t') = \int_{z'=0}^{\ell} \int_{r'=0}^{r_1} r' R_0(\beta_m, r') Z(\eta_p, z') g(t') dr' dz'. \quad (3a)$$

Also

$$R_0(\beta_m, r) = J_0(\beta_m r), \quad (3b)$$

where  $J_0$  is the Bessel function,  $\beta_m, \eta_p$  are the subsequent roots of equations which will be discussed later (i.e. eqs (3d) and (3g)) and the Norm is

$$\frac{1}{N(\beta_m)} = \frac{1}{N_m} = \frac{2k^2 \beta_m^2}{r_0^2 J_0(\beta_m r_0) (h_e^2 + k^2 \beta_m^2)}. \quad (3c)$$

By using convection boundary condition, the roots can be obtained from [12]:

$$h_e J_0(\beta_m r_0) - k \beta_m J_1(\beta_m r_0) = 0, \quad (3d)$$

where  $J_0, J_1$  are Bessel functions. Newton–Raphson method was used to obtain successive values of the roots (i.e.  $\beta_m$  where  $m$  varies from 1 to infinity). For convection boundary conditions at the facets of the rod, assuming equal convection heat transfer coefficients at both ends of the rod, the value of  $Z(\eta_p, z)$  in eq. (3) can be written as

$$Z(\eta_p, z) = \eta_p \cos(\eta_p z) + H \sin(\eta_p z). \quad (3e)$$

Here as suggested by ref. [13],  $H$  is equal to  $h_a/k$ , where  $h_a$  is the convection heat transfer coefficient from rod facets and for naturally cooled facets,  $h_a$  is equal to  $27.5 \text{ W/m}^2 \cdot \text{K}$  [13].

The Norm can be written as

$$\begin{aligned} \frac{1}{N(\eta_p)} &= \frac{1}{N_p} = \frac{2}{(\eta_p^2 + H^2) (l + [H/(\eta_p^2 + H^2)]) + H} \\ &= \frac{2}{l(\eta_p^2 + H^2) + 2H} \end{aligned} \quad (3f)$$

and the roots can be obtained from

$$\tan(\eta_p l) = \frac{2\eta_p H}{\eta_p^2 - H^2}, \quad (3g)$$

where the Newton–Raphson method is used to obtain successive values of the roots.

The main equation of the solution can be written as:

$$\begin{aligned} \theta = T - T_\infty = & \sum_{m=1}^{\infty} \sum_{p=1}^{\infty} \frac{J_0(\beta_m r)(\eta_p \cos(\eta_p z) + H \sin(\eta_p z))}{N_m N_p} \\ & \times \exp\left(-\frac{k}{\rho c} (\beta_m^2 + \eta_p^2) t\right) \\ & \times \left[ \frac{1}{\rho c} \int_{\tau=0}^{\tau} \exp\left(\frac{k}{\rho c} (\beta_m^2 + \eta_p^2) \tau\right) g(\tau) d\tau \right]. \end{aligned} \quad (4)$$

For Gaussian beam distribution, the function of eq. (3) can be written as

$$\begin{aligned} g(\tau) = & \int_0^{\ell} \int_0^{2w_p} \frac{2\beta\alpha P_{ab}}{\pi w_p^2} \exp\left(\frac{-2r^2}{w_p^2}\right) \\ & \times J_0(\beta_m r) \exp(-\alpha z)(\eta_p \cos(\eta_m z) + H \sin(\eta_p z)) r dr dz. \end{aligned} \quad (5)$$

An old treatise of Bessel function suggested that if the limit of integration is from zero to infinity, then the following integration could be solved [14]:

$$\int_0^{\infty} \exp\left(\frac{-2r^2}{w_p^2}\right) J_0(\beta_m r) r dr = \frac{w_p^2}{4} \exp\left(-\frac{\beta_m^2 w_p^2}{8}\right). \quad (6)$$

It is to be noted that the magnitude of integration is the same when the upper limits of integration is  $2w_p$  or greater up to infinity since in this range no change in the absorbed power will be seen. This is due to the fact that the first term on the left-hand side of eq. (6) will vanish as it increases toward  $2w_p$  and beyond. This is also confirmed by carrying the integration numerically.

The integration in  $z$  coordinate can be solved directly as

$$\begin{aligned} & \int_0^{\ell} \exp(-\alpha z)(\eta_p \cos(\eta_m z) + H \sin(\eta_p z)) dz \\ & = \frac{\eta_p}{\alpha^2 + \eta_p^2} [\exp(-\alpha \ell)(\eta_p \sin(\eta_p \ell) - \alpha \cos(\eta_p \ell) + \alpha] \\ & \quad + \frac{H}{\alpha^2 + \eta_p^2} [\exp(-\alpha \ell)(-\alpha \sin(\eta_p \ell) - \eta_p \cos(\eta_p \ell) + \eta_p] \\ & = A_{mp}. \end{aligned} \quad (7)$$

Combining the results of integrations into eq. (5), the function of eq. (3a) can be written as

$$g(\tau) = \frac{\beta\alpha P_{ab} A_{mp}}{2\pi} \exp\left(\frac{-\beta_m^2 w_p^2}{8}\right). \quad (8)$$

Assuming CW mode then at a time less than or equal to the time necessary to reach the steady-state operation condition, the transform of time ( $\tau$ ) is equal to  $t$  in eq. (4). Incorporating these values in the main solution (i.e. eq. (4)), carrying the time integration then:

$$\begin{aligned} \theta &= T - T_{\infty} \\ &= \frac{\alpha H_f P_{ab}}{2\pi k} \sum_{m=1}^{\infty} \sum_{p=1}^{\infty} A_{mp} \exp\left(-\frac{\beta_m^2 w_p^2}{8}\right) \\ &\quad \times \frac{J_0(\beta_m r) (\eta_p \cos(\eta_p z) + H \sin(\eta_p z))}{N_p N_m (\beta_m^2 + \eta_p^2)} \\ &\quad \times \left[ 1 - \exp\left(-\frac{k}{\rho c} (\beta_m^2 + \eta_p^2) t\right) \right]. \end{aligned} \quad (9)$$

This equation represents the transient temperature distribution through a laser rod that is convection cooled from the edge and its facets and it is assumed that it is valid as long as the time is less than or equal to the time necessary to reach thermal equilibrium. Twenty roots are sufficient to predict the precise value of temperature. Transient solution can also be obtained starting from the rest and the time necessary to reach steady-state operation condition can be obtained. For the solution above, the temperature history in the laser rod can be obtained until the steady-state condition is reached.

As the laser rod is heated because of the part of the absorbed power that is converted to heat, there will be a temperature increase in it which will induce thermal stresses. Since the laser rod is symmetric, the thermal stress distribution can be obtained depending on heat flexibility theory, stress balance equation, geometry equation and generalized Hooke equation of stress distortion [15].

$$\sigma_{rr} = \frac{\gamma E}{1 - \nu} \left( \frac{1}{r_0^2} \int_0^{r_0} \theta r dr - \frac{1}{r^2} \int_0^r \theta r dr \right), \quad (10)$$

$$\sigma_{\theta\theta} = \frac{\gamma E}{1 - \nu} \left( \frac{1}{r_0^2} \int_0^{r_0} \theta r dr + \frac{1}{r^2} \int_0^r \theta r dr - \theta \right), \quad (11)$$

$$\sigma_{zz} = \frac{2\gamma E}{1 - \nu} \left( \frac{1}{r_0^2} \int_0^{r_0} \theta r dr - \theta \right), \quad (12)$$

where  $\sigma_{rr}$ ,  $\sigma_{\theta\theta}$ ,  $\sigma_{zz}$  represent the thermal stress (MPa) along the radius, the annulus and the  $z$  direction,  $\gamma$  represents the coefficient of thermal expansion (1/K) and  $E$  is the Young's modulus (MPa). The rod is assumed to be stress-free and not constrained by external forces and the strains of the crystal are related by the generalized Hooke's laws [16]

$$\varepsilon_{rr} = \frac{1}{E} [\sigma_{rr} - \nu(\sigma_{\theta\theta} + \sigma_{zz})] + \gamma\theta, \quad (13)$$

$$\varepsilon_{\theta\theta} = \frac{1}{E} [\sigma_{\theta\theta} - \nu(\sigma_{rr} + \sigma_{zz})] + \gamma\theta, \quad (14)$$

$$\varepsilon_{zz} = \frac{1}{E} [\sigma_{zz} - \nu(\sigma_{rr} + \sigma_{\theta\theta})] + \gamma\theta, \quad (15)$$

where  $\varepsilon_{rr}$ ,  $\varepsilon_{\theta\theta}$ ,  $\varepsilon_{zz}$  represent the thermal strain along the radius, the annulus and the  $z$  directions and  $\nu$  represents the Poisson's ratio. Here a laser rod pumped by a Gaussian beam profile is convectional cooled. The face and the edge convection heat transfer coefficients are varied to obtain their effect on temperature, stress, strain and subsequently OPD. The time required to reach thermal equilibrium was also obtained in each case. Admitted to represent failure stress, hoop stress is obtained so that the rod may not reach failure stress meanwhile minimum OPD can be achieved. Assume the un-pumped face is coated to be highly reflective, i.e. being used as a mirror. If the contribution from the thermal stress-induced birefringence is neglected, which is small for most cases [5], then for a paraxial coherent beam propagating in the  $z$  direction over an infinitesimal distance  $dz$ , the OPD for one round-trip is given by [17]

$$\text{OPD}(r) = 2 \left( \int_l \frac{\partial n}{\partial T} \theta(r, z, t) dz + \int_l n \varepsilon_{zz} dz \right). \quad (16)$$

It has been found that the first term of eq. (15) (i.e.  $(1/E)[\sigma_{zz} - \nu(\sigma_{rr} + \sigma_{\theta\theta})]$ ) is very small and can be neglected. This is also confirmed by the usual high value of  $E$ , so the  $z$ -component of strain ( $\varepsilon_{zz}$  can be written as  $\gamma\theta$ ), then the OPD equation can be written as

$$\text{OPD}(r) = 2 \left( \frac{\partial n}{\partial T} + \gamma n \right) \int_l \theta(r, z, t) dz. \quad (17)$$

The limiting stress that must not exceed is the failure stress which is admitted in many references to be the maximum tensile hoop stress that can occur in the medium. Then the transient hoop stress can be written as

$$\begin{aligned} \sigma_{\theta\theta} = & \frac{\alpha H_f P_{ab} \gamma E}{2\pi k(1-\nu)} \sum_{m=1}^{\infty} \sum_{p=1}^{\infty} A_{mp} \exp\left(-\frac{\beta_m^2 w_p^2}{8}\right) \\ & \times \frac{[\eta_p \cos(\eta_p z) + H \sin(\eta_p z)] B}{N_p N_m (\beta_m^2 + \eta_p^2)} \\ & \times \left[ 1 - \exp\left(-\frac{k}{\rho c} (\beta_m^2 + \eta_p^2) t\right) \right], \end{aligned} \quad (18)$$

where

$$B = \frac{J_1(\beta_m r_0)}{\beta_m r_0} + 0.5 [J_2(\beta_m r) - J_0(\beta_m r)]$$

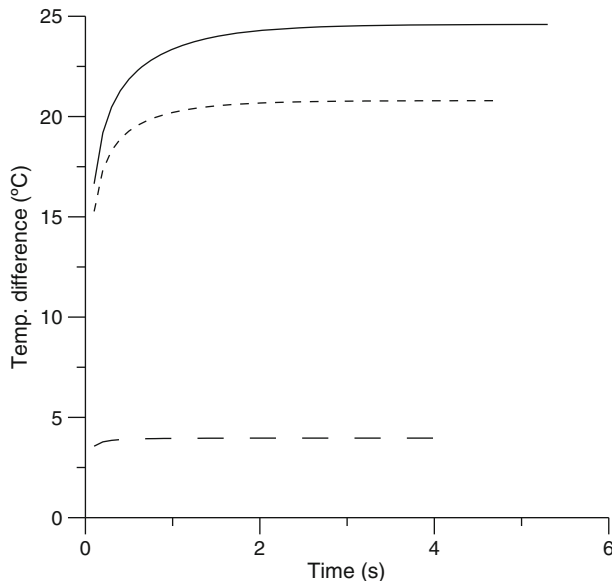
and  $J_0$ ,  $J_1$ ,  $J_2$  are Bessel functions

### 3. Result and discussion

Before trusting the suggested analytical solution, the result obtained from this work was compared with a numerical solution. Many numerical works studied the influence of facets convectional heat transfer on beam distortion, but till now, no analytical solution studied the transient thermal effect on laser rod that is cooled from its facets and edge. Here an analytical solution of transient temperature distribution through the convectional end-pumped laser rod was derived using integral transform method. The steady-state temperature distribution through the rod was also obtained. By comparing the result obtained

from this work for the same laser rod and boundary conditions and that obtained from the numerical solution of ref. [17], an acceptable result was obtained where a maximum difference of 3.5% was observed, assume the thermal and optical properties of this type of crystal are taken from ref. [17] and that the Gaussian beam waist is equal to  $430 \mu\text{m}$ .

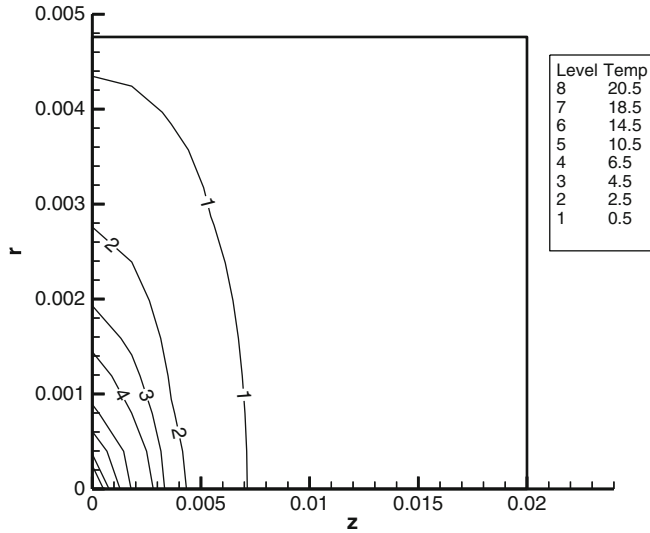
Having solved the temperature distribution in the laser rod using convectonal boundary condition, all other possible boundary conditions on the laser rod can easily be simulated. For example, insulated facets laser rod can be simulated by reducing convection heat transfer coefficient much beyond the convection heat transfer of the naturally cooled facets which is assumed to be equal to  $27.5 \text{ W/m}^2\cdot\text{K}$ . Another example is the possibility of changing the value of edge convection heat transfer coefficient that cooled the laser rod where a zero boundary condition between the lateral side of the laser rod and the cooling fluid can be simulated by increasing the convection heat transfer to  $75 \text{ kW/m}^2\cdot\text{K}$  [17] and beyond where almost zero temperature difference can be achieved. Equation (9) represents the transient temperature distribution through a laser rod that is convectonal cooled from the edge and its facets. For the solution above, the temperature history in the laser rod can be obtained until the steady-state condition was reached. The face temperature history at the centre of the pumped face is shown in figure 2. It shows that the higher the facet cooling (i.e. high edge convection heat transfer coefficient), the lesser the temperature that can be reached in the laser rod and the lesser the time required to reach the thermal equilibrium. This is due to the high rate of heat transfer out of the rod leading to the reduction of the overall temperature distribution as the face cooling is increased.



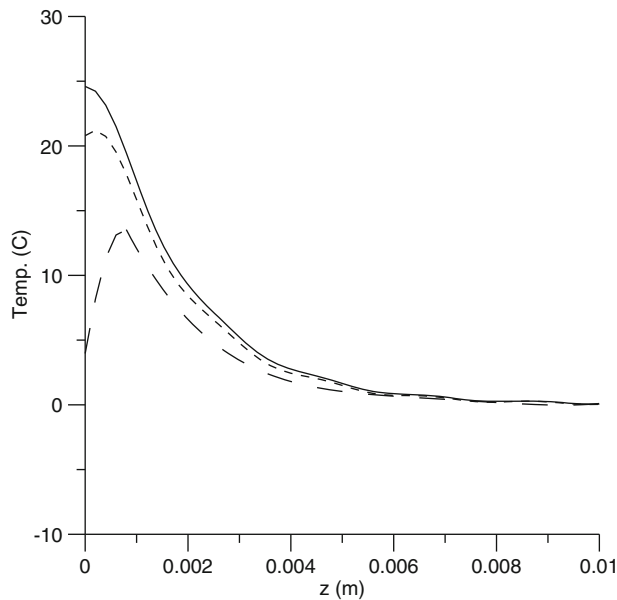
**Figure 2.** The variation of transient temperature with face-cooled facets. Solid line is for  $h_a = 27.5 \text{ W/m}^2\cdot\text{K}$ , small dashed line is for  $h_a = 2700 \text{ W/m}^2\cdot\text{K}$  and long dashed line is for  $h_a = 75000 \text{ W/m}^2\cdot\text{K}$ . The edge-cooled heat transfer coefficient is kept at  $75000 \text{ W/m}^2\cdot\text{K}$ .



Convictional cooled end-pumped laser rod



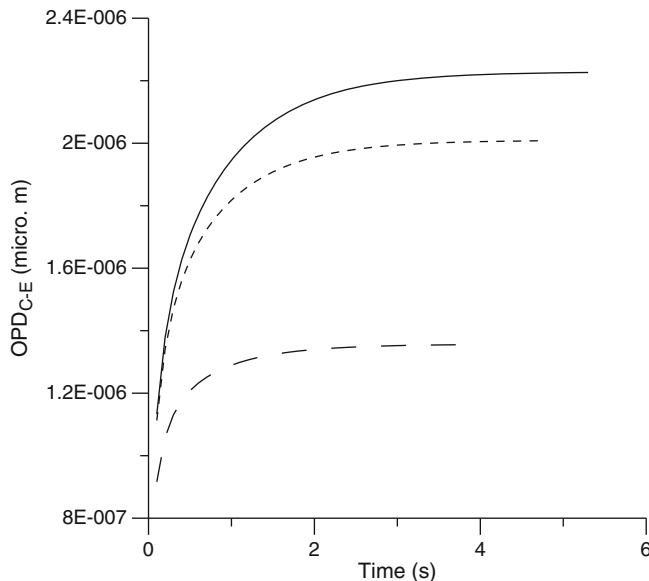
**Figure 3.** Temperature distribution ( $\theta$ ) in the laser rod, assume  $h_a=27.5 \text{ W/m}^2\cdot\text{K}$ ,  $h_c=75000 \text{ W/m}^2\cdot\text{K}$ , that left-pumped by Gaussian beam having a waist radius of  $430 \mu\text{m}$  at the centre of the rod. Assume that the  $z, r$  coordinates are in metre and the max. temperature difference is  $25^\circ\text{C}$ .



**Figure 4.** The variation of the longitudinal temperature at the rod axis with face-cooled heat transfer coefficient. Solid line is for  $h_a = 27.5 \text{ W/m}^2\cdot\text{K}$ , small dashed line is for  $h_a = 2700 \text{ W/m}^2\cdot\text{K}$  and long dashed line is for  $h_a = 75000 \text{ W/m}^2\cdot\text{K}$ . The edge-cooled heat transfer coefficient is kept at  $75000 \text{ W/m}^2\cdot\text{K}$ .

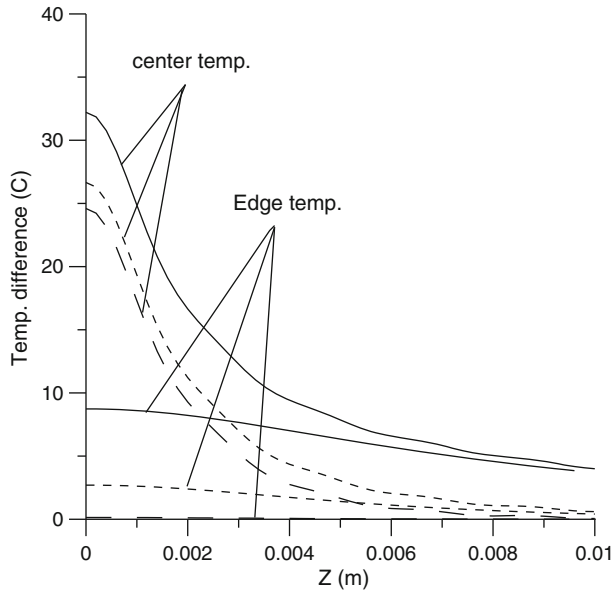
Figure 3 is a graph showing the temperature difference contour through the laser rod where a contour number and what is represented in °C are shown at steady-state condition which is very similar in magnitudes and locations to that given in ref. [13]. The  $r$  and  $z$  coordinates are not drawn to scale so as to indicate the temperature distribution more clearly. Figure 4 shows the longitudinal variation of temperature through the axis of the rod where the edge cooling heat transfer coefficient is kept at  $75000 \text{ W/m}^2\cdot\text{K}$ . The solid line is for face cooling where heat transfer coefficient is  $27.5 \text{ W/m}^2\cdot\text{K}$  and as this coefficient increases, the face temperature decreases due to the increase in the rate of heat transfer through the rod face. The small dashed line indicates the temperature distribution through the laser axis for face cooling where the heat transfer coefficient is increased to  $2700 \text{ W/m}^2\cdot\text{K}$ . The maximum temperature seems to occur deep within the rod because of the high transfer rate of heat outside the rod face. This phenomenon is more clearly seen as the convection heat transfer coefficient increases as shown by the large dashed line that shows the temperature distribution in the rod that has an edge convection heat transfer of  $75000 \text{ W/m}^2\cdot\text{K}$  where the maximum temperature through the rod occurred in more in-depth distance in the rod axis due to the increase in the facially extracted heat.

Figure 5 shows the history of  $\text{OPD}_{c-e}$  (optical path difference between the centre and the edge) with the increase in face cooling. It shows that the higher the facet cooling (i.e. high facet convection heat transfer coefficient), the less is the OPD that can be reached through the laser rod and the less is the time required for the rod to reach its thermal equilibrium. Again, this is due to the high rate of heat transfer out of the rod where a high temperature cannot be established.



**Figure 5.** The variation of transient OPD with face-cooled heat transfer coefficient. Solid line is for  $h_a = 27.5 \text{ W/m}^2\cdot\text{K}$ , small dashed line is for  $h_a = 2700 \text{ W/m}^2\cdot\text{K}$  and long dashed line is for  $h_a = 75000 \text{ W/m}^2\cdot\text{K}$ . The edge-cooled heat transfer coefficient is kept at  $75000 \text{ W/m}^2\cdot\text{K}$ .

Convective cooled end-pumped laser rod



**Figure 6.** The variation of the longitudinal temperature at the rod axis and edge with edge-cooled heat transfer coefficient. Solid line is for  $h_e = 500 \text{ W/m}^2\cdot\text{K}$ , small dashed line is for  $h_e = 2700 \text{ W/m}^2\cdot\text{K}$  and long dashed line is for  $h_e = 75000 \text{ W/m}^2\cdot\text{K}$ . The face-cooled convection heat transfer coefficient is kept at  $27.5 \text{ W/m}^2\cdot\text{K}$ .

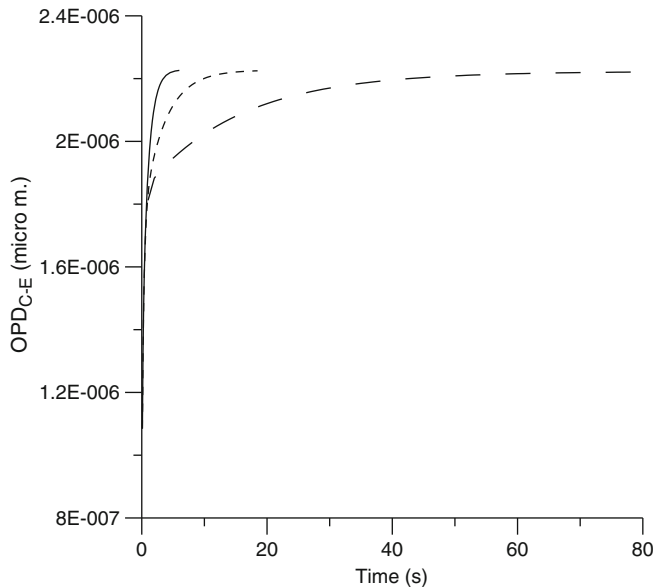


**Figure 7.** The variation of transient  $\text{OPD}_{C-E}$  with edge heat transfer coefficient. Solid line is for  $h = 75000 \text{ W/m}^2\cdot\text{K}$ , small dashed line is for  $h = 2700 \text{ W/m}^2\cdot\text{K}$  and long dashed line is for  $h = 500 \text{ W/m}^2\cdot\text{K}$ . The face-cooled heat transfer coefficient is kept at  $27.5 \text{ W/m}^2\cdot\text{K}$ .

**Table 1.** The effects of varying edge and face cooling of laser rod on temperature, OPD, maximum hoop stress and response time that obtained analytically. ( ) indicates the result as obtained by [13], single asterisk indicates the result obtained by finite element method of this work, double asterisk indicates the result verified by the finite element solution of this work.

$h_a$ (W/m <sup>2</sup> ·K)	$h_e$ (W/m <sup>2</sup> ·K)	Max temp. (°C)	OPD <sub>c-e</sub> (μm)	Max hoop stress (Mpa)	Response time (s)
27.5	75000	24.6** (26)	2.21** (2.2)	9.25** (11)	5.6
2700	75000	20.7*	2*	12.5*	4.8
75000	75000	13.5** (13)	1.3** (1.1)	21.6** (22)	3.8
27.5	2700	26.5	2.21	8.05	20
27.5	500	32	2.21	7.23	80

Figure 6 shows the axial temperature distribution through the axis and the edge of the laser rod for different values of edge cooling convection heat transfer coefficient. It shows that as the convection heat transfer decreases, the temperature distribution increases because of the reduction in the lateral heat transfer out of the rod. The differences between the edge and the centre temperatures are kept approximately constant as the edge-cooled heat transfer coefficient changed which can be explained since an increase in the rod axis temperatures will be combined by an increase in the edge temperature which yields approximately constant difference between them. This prediction leads to an important conclusion where eq. (17) predicts that the OPD depends mainly on the temperature difference between the edge and the centre temperature and since these values are not changed while changing edge-cooled heat transfer coefficient then one can conclude that OPD is independent of edge cooling coefficients. This conclusion is confirmed by the result obtained from this work which is shown in figure 7. It shows that the increase in the edge cooling convection heat transfer coefficient has insignificant effect on the OPD<sub>c-e</sub>, but it significantly reduces the time of thermal response. Then one can say that the edge cooling is not important unless another factor appears. It is the failure stress which must not exceed so as to ensure a safe operation condition.

Using constant convection heat transfer coefficient of the naturally cooled facets which is found to be equal to 27.5 W/m<sup>2</sup>·K and varying the edge cooling convection heat transfer coefficient from 500 to 75000 W/m<sup>2</sup>·K, as shown in table 1, the history of the maximum temperature that can occur through the laser rod (i.e. at the end centre of the pumped facet) is illustrated. It shows that the maximum temperature distribution increases as the edge cooling decreases. The response time also is increased. This is due to the decrease in the rate of heat transfer out of the rod edge as the heat transfer coefficient decreased. A summary of the results are given in table 1.

Since neither plain stress ( $\sigma_{zz} = 0$ ) nor plain strain ( $\epsilon_{zz} = 0$ ) approximations are valid for very high face-cooled laser which are also assumed a constant load (thermal load) throughout the rod [18] which is not the case for high face-cooled laser rod then the finite element method was used to predict the maximum hoop stress that can occur in the laser rod. The reader is referred to [2] for the theory and method of modulation in using finite element method for the laser rod to simulate the case where its results were also verified

by the results of ref. [17]. The result of using finite element method for this work was indicated by asterisks in table 1, which shows good agreement with the results given in ref. [17] and the analytical solution derived in this work.

#### 4. Conclusion

The transient analytical solution of thermal effect in convective cooled end-pumped laser rod was derived. The results were compared with numerical solutions and good agreements were found. The effects of changing the values of edge and face cooling were studied. It is found that increase in the edge cooling results in the reduction of the maximum temperature that can be reached in the laser rod. The increase in this type of cooling also reduces significantly the time required to reach thermal equilibrium and it has no effect on the value of optical path difference. But there is a slight increase in the max. tensile hoop stress that can be reached as edge cooling increases. It was also found that increase in face cooling reduces the response time, optical path difference and the maximum temperature that can be reached in the laser rod. This type of cooling was found to significantly increase the max. tensile hoop stress that can be reached in the laser rod. A matching between the advantages of these two types of cooling may be useful for a designer to design a system that has the possibility of working near failure hoop stress that ensure high possible output power with minimum OPD and has a small response time.

#### References

- [1] Y W Ma and Y Q Chen, *Laser devices* (Zhejiang University Press, Hangzhou, 1994)
- [2] K S Shibib *et al*, *Thermal Sci.* **15**(Suppl. 2), S399 (2011)
- [3] Khalid S Shibib *et al*, *Pramana – J. Phys.* **79**, 287 (2012)
- [4] W Koechner, *Solid-state laser engineering*, 6th edn (Springer Series in Opt. Sci., USA, 2006)
- [5] Peng Shi *et al*, *Photonics and optoelectronics symposium* (2009) pp. 1–4
- [6] E H Bernhardt *et al*, *Opt. Express* **16**, 11115 (2008)
- [7] Y Tian *et al*, *Appl. Phys. B* **103**, 107 (2011)
- [8] Feng Huang *et al*, *Proc. SPIE* **6823**, 682311-1 (2007)
- [9] Khalid S Shibib *et al*, DOI: [10.2298/TSCI110701137S](https://doi.org/10.2298/TSCI110701137S); *Thermal Sci.* (2011) (accepted)
- [10] F P Incropera, D P Dewitt, T L Bergman and S Lavine, *Fundamentals of heat and mass transfer*, 6th edn (John Wiley & Sons, UK, 2007)
- [11] Ananada K Cousins, *IEEE J. Quantum Electron.* **28**, 1057 (1992)
- [12] M N Özisik, *Heat conduction* (Wiley, New York, 1980)
- [13] J Frauchiger, P Albers and H P Weber, *IEEE J. Quantum Electron.* **28**, 1046 (1991)
- [14] G N Watson, *A treatise on the theory of Bessel functions*, 2nd edn (Cambridge University Press, London, 1966) 393
- [15] Ping Xiuer, *Thermal stress and thermal fatigue* (National Defence Industry Press, Beijing, 1984)
- [16] Zhing Li, Xiulan Huai and Li Wang, *Appl. Therm. Eng.* **29**, 2927 (1991)
- [17] C Pfister, R Weber, H P Weber, S Merazzi and R Gruber, *IEEE J. Quantum Electron.* **30**, 1605 (1994)
- [18] S P Timoshenko and J N Goodier, *Theory of elasticity*, 3rd edn (McGraw-Hill, New York, 1970)